JOURNAL OF MAGNETIC RESONANCE **125,** 107–113 (1997)
ARTICLE NO. MN961045

X-Band EPR Study of an Unusual Center in X-Irradiated Zircon at 10 K

R. F. C. CLARIDGE, G. L. A. SUTTON, AND W. C. TENNANT

Chemistry Department, University of Canterbury, Private Bag 4800, Christchurch, New Zealand

Received September 5, 1996; revised October 17, 1996

Observation by EPR at 8.9 GHz and approximately 10 K and spin-Hamiltonian analysis of two stable paramagnetic centers in zirconium silicate is reported. The centers are formed by X irradiation at 77 K, and observed after cold transfer to the EPR cavity. Although the centers may be treated as independent, they can best be described as a triradical species formed between two oxygen-trapped hole centers and a trapped electron. The coupling between the holes and electron is apparently ferrimagnetic in nature with a scalar J coupling constant around 23 cm^{-1}.

INTRODUCTION

In a previous paper in this series (*1*), the observation of two oxygen-trapped hole centers formed when zircon is irradiated with X rays at 77 K and transferred cold to the EPR spectrometer cavity was described and the spin-Hamiltonian analysis given. The first of these, labeled D, decayed irreversibly when the crystal was warmed while the second, labeled RT, was found to be stable after warming to room temperature; both were studied at approximately 10 K at X-band frequencies. They were found to exhibit monoclinic symmetry and were assigned to a ligand oxygen atom with their g-tensor principal directions related by a 17.8° rotation about the crystal b axis. A Zr^{3+} spectrum was also described and analyzed in (*1*). In two later papers, an oxygen-hole $[AlO_4]^0$ species (*2*) and a d^1 Ti^{3+} species (*3*) were described. The current spectrum, labeled C, formed by X irradiation at 77 K, cold transfer to the EPR cavity, and subsequent warming to room temperature, is shown in relation to the other centers in Fig. 1 of (*1*).

The C center has defied explanation for some time because of its obvious stability and high symmetry—the g factor for the center is 1.9993 and almost isotropic. In a tetragonal crystal where uniaxial, or lower, symmetry is readily apparent for all of the centers hitherto studied, this was unusual. A weaker but related center which is designated Z is also observed. In contrast to C, the Z center is highly anisotropic.

EXPERIMENTAL

Details of the Varian E12 spectrometer and the crystal goniometer are as described earlier (*1*). The crystal was cut accurately to a parallelepiped (3.5 × 5.5 × 2.0 mm) with faces parallel to the crystallographic a, b, and c axes of the tetragonal (space group $I4_1/amd$) crystal system. The crystal was irradiated at 77 K with X rays from a W tube and transferred cold to the previously cooled Displex head of the cavity goniometer system. The alignment of the crystal was confirmed by observing the previously determined $Zr^{3+}(\alpha)$ and $[AlO_4]^0$ centers, each of which collapses from three symmetry-related species in planes containing the tetragonal axis to a single species for $\mathbf{B}\|\mathbf{c}$. The Displex cooler was then turned off and the cavity filled with helium gas for efficient heat transfer. The crystal was allowed to warm for one hour to near room temperature to anneal the prominent $Zr^{3+}(\alpha)$, the $[AlO_4]^0$ hole center, and other unstable centers. Following this treatment the cavity was cooled to around 10 K for further EPR measurements.

The spectrum then consists, in the main, of two strong centers, the Ti^{3+} center previously described (*3*) and the C center, and one weaker center labeled Z. For the analysis of the C and Z centers, the smallness of some hyperfine splittings and small differences between spectra of symmetry-related species made it necessary to carry out measurements in five distinct crystal planes: bc, ab, and ac and two planes containing **c** obtained by rotating from the ac plane 30° and 45° respectively about the c axis. Hereafter these two planes are referred to simply as the 30° and 45° planes. A good representation of data for spin-Hamiltonian (SH) analysis of the centers was selected from two or three planes so that in each case the parameter matrices were well overdetermined. Measurements were carried out at 5°–10° angular intervals in the planes. Angles were determined to within 2 minutes of arc. The magnitude of the magnetic field was measured with a Bruker NMR gaussmeter to ±0.002 mT and the microwave frequency with a Systron Donner 6016 counter to ±1 kHz.

EXPERIMENTAL RESULTS

Along the c axis the C center was observed (Fig. 1) as a strong, almost isotropic, center line with g factor 1.99925 ± 0.00001, flanked by four pairs of hyperfine lines with splittings for the outer pair around 0.6 mT. Relative intensities and subsequent fitting of the angular dependencies of these lines led to the conclusion that the

1090-7807/97 $25.00

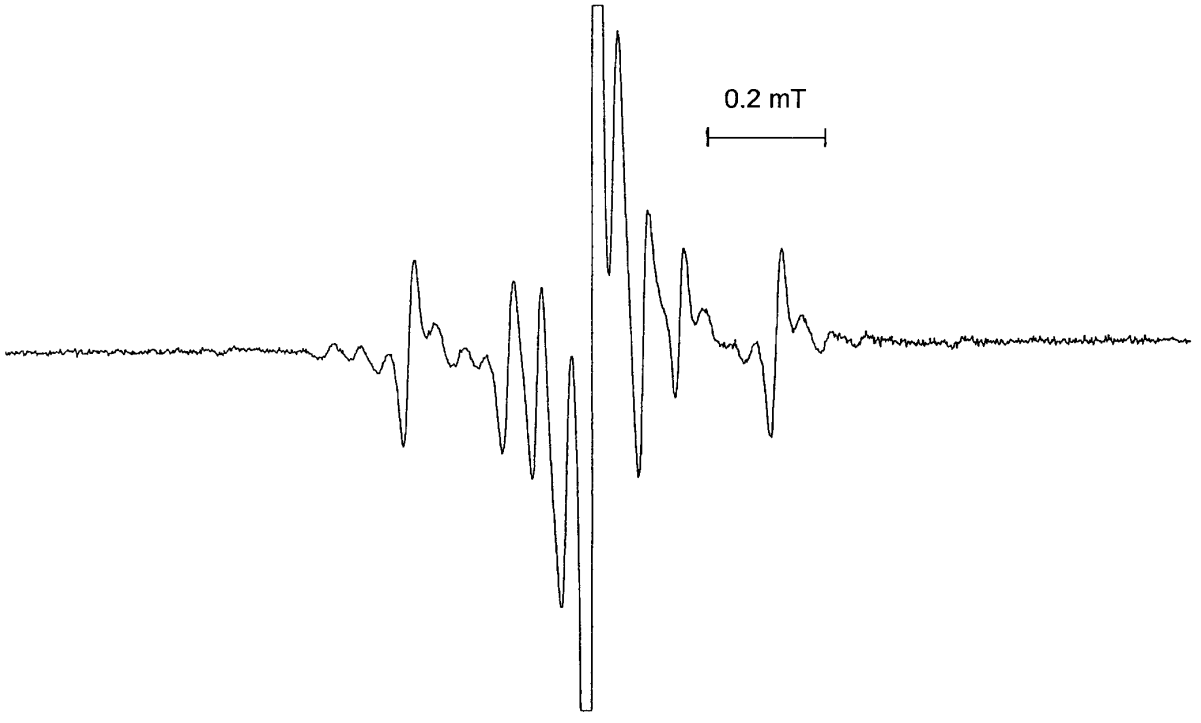

FIG. 1. The *c*-axis spectrum of the C center at 10 K and frequency 8.9 GHz.

outer pair arises from ^{29}Si ($I = \frac{1}{2}$, relative abundance 4.6%) hyperfine interaction and the inner six lines arise from ^{91}Zr ($I = \frac{5}{2}$, relative abundance 11.2%) hyperfine interaction. Observed peak-to-peak linewidths are around 0.02 mT and independent of crystal orientation.

Also observed, but not apparent in Fig. 1, was a second anisotropic line (labeled herein as the Z center) which, within experimental error, coincided with the C-center line with **B** along the *c* axis. The effective, near uniaxial, *g* factors for this anisotropic line are $g_\parallel = 1.9991 \pm 0.0001$ and $g_\perp = 3.9118 \pm 0.0001$. This line is also flanked by four pairs of hyperfine lines with the same pattern as the C center, but with splittings around a factor of six larger. The peak-to-peak linewidths are approximately 0.08 mT and almost independent of crystal orientation.

The C and Z centers are both stable to warming to room temperature but only appear at temperatures below 77 K. Concomitant with the appearance of C and Z centers as the temperature is lowered is the disappearance of the RT oxygen-hole center. This arises because of the different saturation characteristics of the two species: RT is observed only with microwave power less than about 0.05 mW. In general C and RT cannot be observed simultaneously. Both C and Z have the same saturation characteristics, being unobservable for microwave power below about 0.01 mW.

DISCUSSION

(a) The Origin of the C and Z Centers

Since the C and Z centers have the same temperature and power-saturation characteristics and have in common one of their *g*-tensor principal directions, that along the crystal *c* axis, the proposition that both sets of lines arise from the same paramagnetic system needs to be examined. The effective *g* values for the Z center, $g_\parallel \approx 2$ and $g_\perp \approx 4$, are characteristic of a quartet, $S = \frac{3}{2}$, spin system with a large tetragonal distortion (*4*). Possible transition metal ion candidates are d^3 Cr^{3+} or d^3 Mo^{3+}, the former because of its ubiquity and the latter because the zircon crystal was prepared from a melt of lithium molybdate (*5*). However, these ions can be eliminated from consideration because the observed hyperfine splittings are too small and the observed intensity ratios are not in accord with either ^{53}Cr ($I = \frac{3}{2}$) or ^{95,97}Mo ($I = \frac{5}{2}, \frac{5}{2}$) nuclear spins. It should also be noted that Mo^{3+} would be an unexpected oxidation state in zircon. An EPR spectrum of d^1 Mo^{5+} has however been observed in zircon (*6*). A quartet system, possibly arising from O^+, has been reported in neutron-irradiated scheelite (*7*), but the spectrum bears little or no resemblance to that observed here.

A quartet spin system can also arise from pairwise antiferro- or ferrimagnetic coupling of a spin triplet and a spin doublet or, almost equivalently, coupling of a three-spin, $S = \frac{1}{2}$, species (*8*). In the latter case a quartet and two doublets are produced; their ordering depends on the signs and magnitudes of the *J* coupling constants.

Consider a three-spin system $S_1 = S_2 = S_3 = \frac{1}{2}$ and two limiting cases of *J* coupling constants: (i) $J_{12} = J_{13} = J_{23} = J$ and (ii) $J_{12} = J_{13} = J$; $J_{23} = 0$. These are illustrated schematically in Fig. 2 for (a) antiferromagnetic coupling and (b) ferrimagnetic coupling. As discussed in (*9*), anisot-

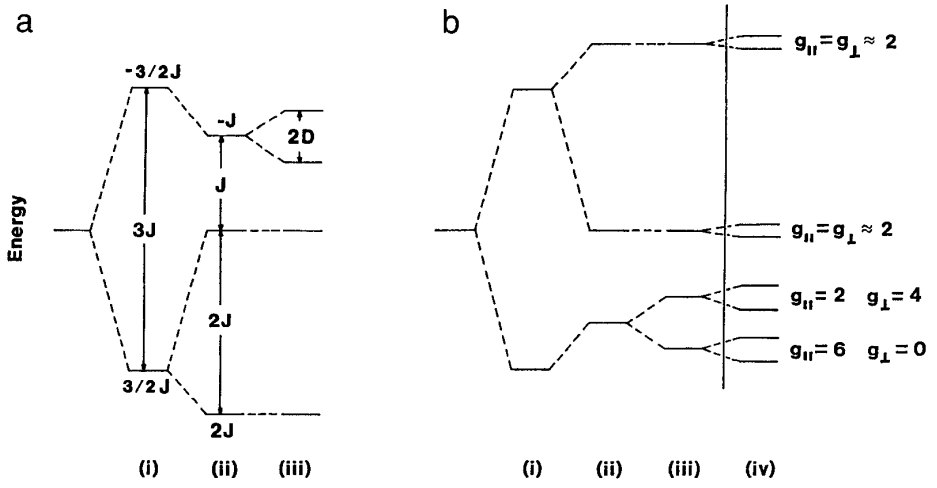

FIG. 2. Energy levels for the proposed triradical: (a) antiferromagnetic coupling and (b) ferrimagnetic coupling (see Discussion for details). The magnetic splittings at the right of (b) are vertically exaggerated by a factor of four for clarity.

ropy in the coupling matrix **J**, equivalent to the presence of a second-degree fine structure matrix **D**, raises the degeneracy of the spin quartet, leading to fine-structure splitting ($=2D$). Provided that the splittings are all large compared to the microwave energy, the four doublets will behave independently, each with its characteristic set of g values. For the two doublets of the spin quartet the g values, for large D, are $g_\parallel = 2$, $g_\perp = 4$ and $g_\parallel = 6$, $g_\perp = 0$. The ordering of the quartet doublets depends on the sign of D. For the other two doublets of the triradical, the values are $g_\parallel \approx g_\perp \approx 2$. Relative intensities will depend upon both the EPR transition probabilities and the Boltzmann spin populations of the various doublets. In X band, the doublet with $g_\parallel = 6$, $g_\perp = 0$ is effectively EPR silent because there is only a finite transition probability when a component of $g_\parallel$ lies along the microwave field direction and, at X-band frequencies, all resonant fields lie at inaccessibly high static field values.

(b) Spin-Hamiltonian Analysis

Throughout this work the program EPR-NMR (*10*) and its predecessor EPR has been used. The spectra of the C and Z centers were analyzed in several different ways as follows.

(i) As separate centers. The SH

$$(H_S)_j = \sum_j [\beta_e \mathbf{B}\cdot\mathbf{g}\cdot\mathbf{S} + \sum_i \{\mathbf{I}\cdot\mathbf{A}_i\cdot\mathbf{S} + \mathbf{I}\cdot\mathbf{P}_i\cdot\mathbf{I} - \beta_N\mathbf{B}\cdot(\mathbf{g}_N)_i\cdot\mathbf{I}\}] \quad [1]$$

was used to analyze each of the centers separately. For the center line of the C center (spinless isotopes), the second summation of terms in Eq. [1] was omitted. The spinless line of the Z center was treated initially as a spin $S_{\text{eff}} = \frac{1}{2}$ system and then, following the arguments of the previous section, as a spin $S = \frac{3}{2}$ system. The usual second-degree fine-structure term **S.D.S** needed then to be added to Eq. [1].

For the C center, no site splitting of the central line was observed in any crystal orientation. However, for the outer pair of ^{29}Si hyperfine lines and for the inner sextet of ^{91}Zr hyperfine lines, site splitting corresponding to monoclinic site symmetry was observed: four symmetry-related species in general orientations collapsed to three species in the *bc* and *ac* crystal planes, to two species in the *ab* plane, and to a single species along the crystal *c* axis. In these cases the analysis was over the $j = 1{-}4$ symmetry-related sites (*11*) corresponding to C_4 symmetry. Site splitting would also be expected in the central, spinless isotope, lines but none was observed. Estimated splittings, based on those observed for the outer, ^{29}Si hyperfine lines, are considerably less than the observed linewidth.

For the anisotropic Z center, linewidths were a factor of four broader, and the lines considerably weaker, than those for the C center. The signal-to-noise value and resolution were such that no consistent site splittings could be measured. The center was consequently treated as one with tetragonal site symmetry, although one suspects that, as for the C center, the symmetry was in fact slightly distorted from tetragonal to monoclinic symmetry.

(ii) As a triradical species. In this case (only lines from spinless isotopes treated), following (*9*) the SH was taken as

$$\begin{aligned} H_S = {} & \beta_e(\mathbf{S}_1\cdot\mathbf{g}_1 + \mathbf{S}_2\cdot\mathbf{g}_2 + \mathbf{S}_3\cdot\mathbf{g}_3)\cdot\mathbf{B} \\ & + \tfrac{1}{2}(\mathbf{S}_1\cdot\mathbf{J}_{12}\cdot\mathbf{S}_2 + \mathbf{S}_2\cdot\mathbf{J}_{12}\cdot\mathbf{S}_1) \\ & + \tfrac{1}{2}(\mathbf{S}_1\cdot\mathbf{J}_{13}\cdot\mathbf{S}_3 + \mathbf{S}_3\cdot\mathbf{J}_{13}\cdot\mathbf{S}_1) \\ & + \tfrac{1}{2}(\mathbf{S}_2\cdot\mathbf{J}_{23}\cdot\mathbf{S}_3 + S_3\cdot\mathbf{J}_{23}\cdot\mathbf{S}_2). \end{aligned}$$

From our data, $\mathbf{J}_{23}$ is either zero or indeterminate because we were only able to observe transitions within two doublets. Spins 1 and 2, taken here to represent identical hole centers, are identical and, writing $\mathbf{J}_{12} = \mathbf{J}_{13} = \mathbf{J}$, $\mathbf{J}_{23} = 0$, the spin Hamiltonian reduces to

$$H_S = \beta_e\{\mathbf{S}_1\cdot\mathbf{g}_1 + 2(\mathbf{S}_2\cdot\mathbf{g}_2)\}\cdot\mathbf{B} + 2\{\tfrac{1}{2}(\mathbf{S}_1\cdot\mathbf{J}\cdot\mathbf{S}_2 + \mathbf{S}_2\cdot\mathbf{J}\cdot\mathbf{S}_1)\}. \quad [2]$$

The electron-spin quantum numbers are $S_1 = S_2$ $(=S_3) = \frac{1}{2}$ and the matrices $\mathbf{g}_1$, $\mathbf{g}_2$ $(=\mathbf{g}_3)$, and $\mathbf{J}$ are taken to be symmetric. Matrix $\mathbf{J}$ in Eq. [2] is not traceless; it contains the scalar (isotropic) exchange parameter J as well as the traceless anisotropic part ($\mathbf{D}$) of $\mathbf{J}$ (*9*). Parameters resulting from fitting the C- and Z-center spinless isotope data simultaneously to Eq. [2] are listed in Table 3.

(c) General Discussion

From Table 1 the highly symmetric nature of the C-center lines is apparent. Anisotropy in the g tensor is determinate only because of the very precise directional data collected and subsequent matrix diagonalization analysis of this data. $\mathbf{g}$ is close to uniaxial (uniaxial component $b = [g_1 - \mathrm{Tr}(\mathbf{g})/3] = 0.000026$) with the ''unique'' direction lying along the crystal c axis. Within error, no off-diagonal matrix elements were detected in the g tensors of Table 1. That is, within error, monoclinic symmetry could not be detected in the g tensor alone, and the data are quoted for orthorhombic symmetry with principal axes lying along the crystallographic axes. The g tensor of Table 1(b) is regarded as being more reliable than that of Table 1(a) (although the uncertainties quoted are the same) because it is based upon well-resolved hyperfine components in which site splittings could be easily measured and assigned unequivocally. As noted above, no site splittings could be detected in the spinless isotope lines.

Table 1(b) indicates that the ^{29}Si hyperfine matrix has monoclinic symmetry. The hyperfine splittings are small, and from the tables of Morton and Preston (*12*) the spin density on Si can be only about 1%. Taking the Si atom at fractional coordinates $[0\ 0\ \frac{1}{2}]$ as the hyperfine-matrix origin, two principal directions of the ^{29}Si A matrix are coplanar with two Si–O bonds and the third, as required by crystal symmetry, is directed along the b axis.

From Table 1(c), the magnitudes of ^{91}Zr hyperfine splittings indicate that the trapped electron is not localized in the Zr d orbitals: from Morton and Preston (*12*) [see also data for $Zr^{3+}(\alpha)$ (*1*)], 100% spin density localized in a d orbital would result in hyperfine splittings around 10 mT—i.e., ~200 times the splittings observed here. The hyperfine-matrix principal directions are rotated by 90° about the c axis in comparison to those of the ^{29}Si hyperfine matrix of Table 1(b). With Zr at the origin, [0 0 0], two principal hyperfine directions are coplanar with Zr–O directions. The two O atoms in question are the second pair of O's attached to Si $[0\ 0\ \frac{1}{2}]$ of the preceding paragraph. As discussed later, it is believed that each of these latter two O atoms traps a hole in the formation of the C (and Z) center. The third principal direction of $\mathbf{A}$ lies along $\mathbf{a}$.

Further from Table 1(c), it should be noted that the ^{91}Zr nuclear-electric-quadrupole and nuclear-Zeeman matrices are both well determined. Matrices $\mathbf{A}$, $\mathbf{P}$, and $\mathbf{g}_N$ have in common the crystal a axis, as required by monoclinic site symmetry, but their remaining coplanar principal directions do not coincide—although the maximum noncoincidence is only about 18°. Our experiments do not establish the absolute sign of $\mathbf{A}$ (^{91}Zr). The signs of $\mathbf{P}$, $\mathbf{g}_N$ (^{91}Zr) are known relative to $\mathbf{A}$, which is here assumed positive.

Of particular interest is the g_N matrix. As in the earlier work on d^1 Ti^{3+} (*3*), the g_N matrix has been allowed to vary, within the constraint of monoclinic symmetry. The isotropic component of the matrix, $g_N(\mathrm{iso}) = \mathrm{Tr}(\mathbf{g}_N)/3 = -0.524 \pm 0.030$, is in very good agreement with the accepted isotropic value for ^{91}Zr, -0.521448, found from NMR experiments (*13*).

In (*3*) it was shown that the P and g_N parameter matrices could be influenced significantly by inclusion of high-spin nuclear-Zeeman terms of dimension I^3B, I^5B when $I = \frac{5}{2}$. These terms were included in the present refinements, again within the constraint of monoclinic site symmetry, and a further small diminution of the RMSD, ~6%, was obtained. However, the magnitudes of these parameters were found to be very small and the P and g_N parameter matrices listed in Table 1(c) were only slightly changed. These latter results have not been included.

A further point regarding the ^{91}Zr hyperfine analysis is that the relative magnitudes of the hyperfine, quadrupole, and nuclear-Zeeman interactions meant that there was a fairly complicated mixing of hyperfine levels and considerable difficulty in assigning the level labels. The following procedure was adopted. The ''allowed'' transitions along the c and/or b axis were first assigned and then the ''allowed'' and ''forbidden'' transitions in intermediate crystal orientations were assigned by successive steps of refinement and simulation using program EPR-NMR (*10*). During level-label-assignment refinements, the nuclear g_N value was held constant and isotropic at the accepted, NMR-determined value (*13*) for ^{91}Zr. With the very small hyperfine interaction constants observed, a different initial value of g_N could have led to different level labels. One should be careful therefore not to read too much into the anisotropic g_N matrix of Table 1(c). Nevertheless, there is confidence that the value $g_N(\mathrm{iso}) = -0.524$ found experimentally is good confirmation that the hyperfine structure does indeed arise from ^{91}Zr interaction.

The center designated Z did not lend itself easily to such a complete analysis: the spinless isotopes produced a line reasonably strong but about a factor of four broader than the

TABLE 1
SH Parameters for the C Center[a]

	Matrix **Y**			k	Principal value, Y_k	Principal direction[b] θ_k (°)	Principal direction[b] ϕ_k (°)
(a) Even isotopes, $I = 0$							
	1.999386(2)	0	0				
g		1.999373(3)	0				
			1.999243(1)				
69 unit-weighted data points from *ac*, 30°, 45° planes; RMSD[c] = 0.0009 mT							
(b) Outer hyperfine (^{29}Si) lines, $I = \frac{1}{2}$							
	1.999378(2)	0	0				
g		1.999383(2)	0				
			1.999245(1)				
	0.5474(8)	0	0.0649(5)	1	0.6494(5)	147.5(2)	180
$\mathbf{A}/g_e\beta_e$ (mT)		0.5023(8)	0	2	0.5061(8)	57.5(2)	180
			0.6081(3)	3	0.5023(8)	90	90
	−1.1106	0	0				
$\mathbf{g}_N$[d]		−1.1106	0				
			−1.1106				
784 unit-weighted data points from *ac*, 30°, 45° planes; RMSD = 0.0027 mT							
(c) Inner hyperfine (^{91}Zr) lines, $I = \frac{5}{2}$							
	1.999344(10)	0	0				
g		1.999406(10)	0				
			1.999253(2)				
	0.0413(13)	0	0	1	0.0635(6)	30.2(2.4)	90
$\mathbf{A}/g_e\beta_e$ (mT)		0.0540(12)	0.0055(4)	2	0.0508(9)	120.2(2.4)	90
			0.0603(3)	3	0.0413(13)	90	0
	−0.0026(2)	0	0	1	0.0044(2)	38.5(1.3)	270
$\mathbf{P}/g_e\beta_e$ (mT)		0.0006(2)	−0.0030(2)	2	−0.0018(2)	51.5(1.3)	90
			0.0020(2)	3	−0.0026(2)	90	0
	−0.498(20)	0	0	1	−0.469(8)	20.2(3.3)	90
$\mathbf{g}_N$		−0.590(21)	0.044(6)	2	−0.489(21)	90	0
			−0.485(9)	3	−0.606(19)	110.2(3.3)	90
259 unit-weighted data points from 30° and 45° planes; RMSD = 0.0051 mT							

[a] Error estimates in parentheses.
[b] Angle θ measured from **c** and angle ϕ in an anticlockwise direction from **a**.
[c] RMSD, root-mean-squared deviation.
[d] g_N matrix is held isotropic at the NMR determined ^{29}Si value (refer to text).

C-center line. Hyperfine splitting patterns were as observed for the C center, but the splittings were about a factor of six larger and the observed lines were, in most crystal orientations, very weak. Along the *c* axis, where the two centers apparently coincide, no hyperfine splittings could be measured because of overlapping with the stronger C-center lines. As already mentioned no consistent site splitting could be measured because the resolution and S/N were too poor.

The Z-center lines were refined initially to an $S_{\text{eff}} = \frac{1}{2}$ system and the g and ^{29}Si A matrices were obtained: $g_1 = 3.9128 \pm 0.0001$, $g_2 = 3.9107 \pm 0.0002$, $g_3 = 1.9991 \pm 0.0001$; $A_1 = 3.49 \pm 0.01$, $A_2 = 3.49 \pm 0.01$, $A_3 = 4.71 \pm 0.06$ mT. Here matrix $\mathbf{g}_N$ was set to $-1.1106\mathbf{U}$, where $\mathbf{U}$ is the 3×3 unit matrix. As discussed earlier such results are indicative of a spin quartet, $S = \frac{3}{2}$, system with large tetragonal distortion, and refinement of the Z-center data on this basis are given in Table 2. Because the ZFS is large and because transitions for only one doublet at accessible X-band fields were able to be found, the matrix $\mathbf{D}$ is not well determined.

TABLE 2
SH Parameters for the Z center fitted to a Quartet, $S = \frac{3}{2}$, System[a]

	Matrix **Y**			k	Principal value, Y_k	Principal directions θ_k (°)	Principal directions ϕ_k (°)
(a) Even isotopes, $I = 0$							
	1.9564(3)	0	0	1	1.9993(1)	0.5(1)	270
g		1.9573(2)	−0.0004(1)	2	1.9573(2)	89.5(1)	90
			1.9993(1)	3	1.9564(3)	90	0
	1.51(31)	0	0				
$\mathbf{D}/g_e\beta_e$ (T)		1.51(31)	0				
			−3.03(62)				
73 unit-weighted data points from *ab*, *bc*, 30° planes; RMSD = 0.053 mT							
(b) Outer hyperfine (^{29}Si) lines, $I = \frac{1}{2}$							
	1.9564(2)	0	0				
g		1.9564(2)	0				
			1.9990(2)				
	1.66(49)	0	0				
$\mathbf{D}/t_e\beta_e$ (T)		1.66(49)	0				
			−3.32(97)				
	3.49(1)	0	0				
$\mathbf{A}/g_e\beta_e$ (mT)		3.49(1)	0				
			4.71(4)				
	−1.1106	0	0				
$\mathbf{g}_N$[d]		−1.1106	0				
			−1.1106				
63 unit-weighted data points from *ab*, *bc*, 30° planes; RMSD = 0.038 mT							

[a] Error estimates in parentheses.
[d] See footnote *d* in Table 1.

At this stage, a weak inner sextet of hyperfine lines, which are also believed to arise from ^{91}Zr hyperfine interaction, has not been analyzed. The measured splittings along **c** and **b** respectively suggest $A_\parallel = 0.64$ mT and $A_\perp = 0.50$ mT as reasonable estimates of the principal values.

Finally, as outlined in (a) above, the analysis of the C and Z centers as a triradical species is considered. The result of this analysis is set out in Table 3. In the absence of lines from the second of the two doublets of the triradical system, it is assumed that the coupling is ferrimagnetic in nature. The appropriate ordering of the energy levels is then as depicted in Fig. 2b. The scalar coupling constant J has a value of about 23 cm^{-1} (or 24.4 T in units of $1/g_e\beta_e$), which means that the upper doublet would be only 0.006% populated at 10 K and probably not observable. Such a transition was sought over a range of temperatures, 10–100 K, but no line could be found which could be assigned unequivocally to the upper doublet.

From Table 3 the triradical g values are, within error, almost identical to the corresponding matrices of Tables 1 and 2—i.e., g_1 corresponds to the C-center g matrix and g_2 ($=g_3$) corresponds to the Z-center g matrix. An almost equally good triradical fit is obtained if one simply substitutes the g matrices for the C and Z centers and holds them constant during the refinement.

The matrix **J**, in T, may be decomposed,

$$\mathbf{J}/g_e\beta_e = \begin{bmatrix} -24.4 & 0 & 0 \\ 0 & -24.4 & 0 \\ 0 & 0 & -24.4 \end{bmatrix} + \begin{bmatrix} 3.4 & 0 & 0 \\ 0 & 3.4 & 0 \\ 0 & 0 & -6.8 \end{bmatrix},$$

where the second matrix represents the matrix **D** in the quartet state of the triradical. The parameter D, as defined implicitly in Eq. [2], is just $2D$ in the conventional ZFS term **S.D.S**. Within error the agreement with the matrix **D** of Table 2 is then good.

TABLE 3
SH Parameters for C and Z Centers Fitted to Triradical $S_1 = S_2 = S_3 = \frac{1}{2}$[a] System

	Matrix **Y**		
	1.99939(4)	0	0
$\mathbf{g}_1$		1.99939(4)	0
			1.99929(3)
	1.95771(6)	0	0
$\mathbf{g}_2(=\mathbf{g}_3)$		1.95771(6)	0
			1.99929(3)
	−21.0(1.3)	0	0
$\mathbf{J}/g_e\beta_e$		−21.0(1.3)	0
(T)			−31.3(2.0)

95 unit-weighted data points from *ab*, *bc*, 30° planes: RMSD = 0.028 mT

[a] Error estimates in parentheses.

The location of the supposed triradical is reasonably clear, but the mode of its formation is less certain and there is no reasonable explanation to account for its stability. The symmetry axis of the triradical is certainly the fourfold screw axis of the tetragonal unit cell which contains both Si and Zr atoms. Referred to Zr as origin with fractional coordinates [0 0 0], it is believed that the two holes involved are trapped at O atoms with fractional coordinates [0 0.18 0.32] and [0 −0.18 0.32] (these are the O atoms attached to Si [0 0 $\frac{1}{2}$] referred to earlier) and that the trapped electron with which they interact to form the triradical lies on the 4_1 axis. With regard to mechanism, it has previously been noted that the $Zr^{3+}(\alpha)$ spectrum is annealed as the temperature is raised above about 100 K. Subsequent recooling results in a growth of the C and Z centers. The $Zr^{3+}(\alpha)$ center arises, following irradiation, from an electron being added to the *d* orbitals of a Zr^{4+} ion in the vicinity of a Y^{3+} ion. On warming, the electron is evidently lost from the *d* orbitals but we can assume that it remains localized near the Zr^{4+} ion, presumably trapped by a purely electrostatic interaction; the observed ^{91}Zr hyperfine splittings are far too small for the trapped electron to be located in the Zr orbitals.

The reasons for the high stability of the triradical species are far from clear. The $Zr^{3+}(\alpha)$ spectrum is stable only at temperatures below about 100 K and its observation requires cold transfer to the EPR cavity following irradiation. On warming we would have expected the trapped electron to simply diffuse away from the Zr^{3+}, perhaps to annihilate a nearby oxygen-hole center. A scenario more likely than triradical formation might have been the formation of a biradical [cf. (*9*)], or a two-hole triplet species as observed by Nuttall and Weil (*14*). However, such species have not, so far, been observed in zircon.

REFERENCES

1. R. F. C. Claridge, G. L. A. Sutton, and W. C. Tennant, *J. Phys.: Condens. Matter* **6,** 3429 (1994).
2. R. F. C. Claridge, G. L. A. Sutton, and W. C. Tennant, *J. Phys.: Condens. Matter* **6,** 10415 (1994).
3. R. F. C. Claridge, D. G. McGavin, and W. C. Tennant, *J. Phys.: Condens. Matter* **7,** 9049 (1995).
4. J. R. Pilbrow, *J. Magn. Reson.* **31,** 479 (1978).
5. A. B. Chase and J. A. Osmer, *J. Electrochem. Soc.* **113,** 198 (1966).
6. K. Eftaxias, P. E. Fielding, and G. Lehmann, *Chem. Phys. Lett.* **160,** 36 (1989).
7. P. Weightman, B. Henderson, and D. E. Dugdale, *Phys. Status Solidi B* **49,** 221 (1972).
8. E. Sinn, *Coord. Chem. Rev.* **5,** 313 (1970).
9. J. Isoya, W. C. Tennant, Y. Uchida, and J. A. Weil, *J. Magn. Reson.* **49,** 489 (1982).
10. D. G. McGavin, M. J. Mombourquette, and J. A. Weil, Computer Program EPR-NMR, Department of Chemistry, University of Saskatchewan, Canada, 1995.
11. J. A. Weil, T. Buch, and J. E. Clapp, *Adv. Magn. Reson.* **6,** 183 (1973).
12. J. R. Morton and K. F. Preston, *J. Magn. Reson.* **30,** 577 (1978).
13. P. Raghavan, *At. Data Nucl. Data Tables* **42,** 189 (1989).
14. R. H. D. Nuttall and J. A. Weil, *Can. J. Phys.* **59,** 1886 (1981).